Available online at www.sciencedirect.com
SCIENCE DIRECT®

Journal of the European Ceramic Society 24 (2004) 1129–1133

www.elsevier.com/locate/jeurceramsoc

Spatial distribution of resistive intergranular phase in stabilized zirconia estimated by millicontact impedance spectroscopy

Jong-Heun Lee[a,*], Young-Soo Jung[a], Hyo-Sang Woo[b], Yong-Chae Chung[b], Doh-Yeon Kim[a]

[a]*School of Materials Science and Engineering and Center for Microstructure Science of Materials, Seoul National University, Seoul 151-742, South Korea*
[b]*Department of Ceramic Engineering, Hanyang University, Seoul 133-791, South Korea*

Abstract

The spatial inhomogeneity of a resistive intergranular liquid was estimated by millicontact impedance spectroscopy in a 1-mol%-Al_2O_3-doped 15 mol% calcia-stabilized zirconia specimen. The distribution of the intergranular liquid depended significantly upon the sintering temperature, the cooling rate and the compact density of the green body, which indicates that the present impedance technique is useful for understanding and manipulating the local grain-boundary conduction.

Keywords: Grain boundaries; Impedance; Ionic conductivity; Stabilized zirconia

1. Introduction

Impedance spectroscopy is a useful tool for separating the grain-interior and grain-boundary contributions in many electroceramics.[1] Most analyses have assumed for simplicity that the grain interiors or grain boundaries are electrically homogeneous throughout the specimen.[2,3] However, a specimen under an electric field [4] or with a functionally graded composition [5] may exhibit electrical properties that vary spatially. Rodewald, Fleig and Maier proposed a local impedance technique using an array of micro-scale electrodes. [4,6,7] This technique renders it possible not only to spatially resolve the electrical properties within a large grain but also to directly investigate an individual grain boundary.[7,8] However, the conduction for a single grain boundary can become heterogeneous due to differences in the wetting of a resistive liquid,[9] the liquid distribution,[10] the grain-boundary type (low angle or high angle),[11] boundary microstructure (straight or undulated) etc. Indeed, as an example of an electrically heterogeneous grain boundary, an uneven distribution of a resistive intergranular liquid has been reported in stabilized zirconia.[12,13] In this case, the average impedance for a small volume rather than the impedance for a single grain boundary would be more advantageous in examining the spatial variation in the grain-boundary conduction.

In this study, a local impedance technique using, one-dimensional or two-dimensional array of sub-millimeter-scale electrodes, was used to estimate the spatially heterogeneous distribution of a resistive intergranular liquid. The technique was referred to as 'millicontact impedance spectroscopy'. The results obtained from the calcia-stabilized zirconia (CSZ) containing a small amount of intergranular liquid were used to demonstrate the validity of this technique.

2. Background of the technique

Fig. 1 shows the equipotential contours of single crystal and polycrystalline materials with a highly insulating grain-boundary phase, which were calculated by a universal Finite Element scheme using CFD-ACE software under the appropriate mesh size and boundary conditions. The case for highly conducting grain boundaries was not considered in this study because the grain boundaries in stabilized zirconia are known to be 10^2–10^4 times more resistive than the grain interiors.[13,14] In the calculation, the ac electric field was applied not between a single pair of the opposite electrodes but between all opposite electrodes in order to determine the

* Corresponding author. Tel.: +82-2-880-6891; fax: +82-2-884-1413.
E-mail address: jongheun@snu.ac.kr (J.-H. Lee).

0955-2219/$ - see front matter © 2003 Elsevier Ltd. All rights reserved.
doi:10.1016/S0955-2219(03)00584-3

entire potential distribution. In a single crystal [Fig. 1(a)], the local impedance can be simply measured as a function of the distance between two opposite electrodes. Note that not only does the volume between two opposite electrodes (region A) contribute in the measured impedance but so does the extra volume due to the circumventing conduction path (see the current line in region B) between the electrode edges. However, this extra volume effect will not affect the overall tendency unless the spatial variation of the electrical properties is not large near the edge. Another factor that should be taken into account is that a negligible surface conduction between the near-surface electrodes (1 and 1′ electrodes) is desirable for an estimation of the spatially resolved impedance. For polycrystalline materials with highly resistive grain boundaries [Fig. 1(b)], the equipotential lines near the electrodes in region B become increasingly parallel to the electrode plane, which emanate from the large potential drop across the highly resistive grain boundary phase C. This significantly narrows the circumventing conduction [see the current line of region B Fig. 1(b)]. The extra volume effect would be further diminished for smaller grain size and more resistive grain boundaries. Indeed, the measured impedance between the electrodes 2 and 2′ in CSZ with and without removing the nearby volume [D and E in Fig. 1(b)] were approximately identical, which indicated that the effect of surface conduction and circumventing conduction in this study is negligible.

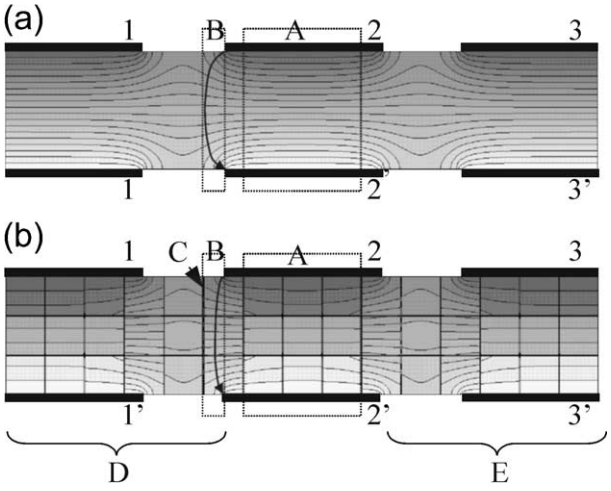

Fig. 1. Equi-potential contour maps of (a) single crystal and (b) polycrystalline materials with highly resistive grain boundary when an ac electric field was applied between the opposite electrodes. The lines and color changes indicate equipotential lines. The potential drop between two neighboring lines is 1/20 of the applied voltage. (grain boundary resistivity) = 100 (grain interior resistivity), (grain boundary thickness) = 0.02 (grain size).

3. Experimental

Calcia-stabilized zirconia (15 mol%; 15CSZ) powder (CSZ-15 Heat-treated, Daiichi Kigenso Kagaku Kogyo Co. Ltd., Osaka, Japan) was used as the raw material. The concentrations of the impurities SiO_2, TiO_2, Fe_2O_3, and Na_2O were 0.04, 0.09, 0.026, and 0.02 wt.%, respectively. After adding 1 mol% of Al_2O_3 (AKP3000, Sumitomo Chemical Co., Tokyo, Japan), the powder mixture was ball-milled for 6 h in ethyl alcohol using partially stabilized zirconia balls. After drying, 7 g of the powder was uniaxially pressed into a cylindrical rod shaped specimen, which was then isostatically pressed at 200 MPa. The compacts were sintered at 1600 or 1650 °C for 4 h in air. The heating rate was fixed at 200 °C/h and two different cooling rates (200 or 800 °C/h) were employed. In order to examine the effect of the sintered density upon the heterogeneity of the intergranular phase, a porous specimen was prepared by sintering without prior isostatic pressing. The detailed conditions for specimen preparation are summarized in Table 1 along with the sample specifications.

An approximately 0.55-mm thick slab was obtained by cutting the sintered specimen along the diameter. The array of rectangular electrodes (area: 2.0 × 0.5 or 0.5 × 0.5 mm^2) was made from the surface to the center with a 0.5 mm spacing by screen printing a Pt paste (TR 7905, Tanaka Co., Tokyo, Japan). After drying, the specimen was heat-treated at 1100 °C for 1 h. In order to measure the local impedance, two opposite electrodes were mechanically contacted with Pt wires with a bead-shape end. An ac two-probe technique by a SI 1260 impedance/gain-phase analyzer (Model No. SI 1260, Solartron, Inc., Farnborough, UK) was used. The data were obtained in an air atmosphere at 400 °C.

4. Results and discussion

A two-dimensional array of the small electrodes was made on both sides of the C1650 specimen, as shown in Fig. 2(a), and the impedance between two opposite electrodes was measured. The complex impedance

Table 1
The specifications, isotatic-pressing parameters, sintering conditions, cooling rates, densities, and average grain sizes(d_g) of the samples

Sample specification	Isostatic pressing	Sintering	Cooling rate	Density (g/cm^3)	d_g[a] (μm)
C1650	Yes	1650 °C for 4h	200 °C/h	5.44	45.2
C1600	Yes	1600 °C for 4h	200 °C/h	5.45	35.1
C1600-FC[b]	Yes	1600 °C for 4h	800 °C/h	5.46	35.0
C1600-LD[c]	No	1600 °C for 4h	200 °C/h	5.27	29.9

[a] Average grain size estimated by linear intercept method.
[b] FC: fast cooling.
[c] LD: low density.

spectra was obtained as a function of the distance from the surface along the axial direction [$x = 5.25$, see the gray arrow in Fig. 2(a)] and are plotted in Fig. 2(b). Three semicircles from the low frequency region represent the contributions of the electrode polarization, the grain boundary, and the grain interior, respectively. The grain-boundary contribution varied significantly from 56 to 3.5 kΩcm with increasing distance from the surface, while the grain-interior resistivity remained constant at 82 kΩcm. Assuming the grain-boundary contribution and thickness is 10 kΩcm and 10 nm, the grain boundary is approximately 500 times more resistive than the grain interior, which is consistent with the literature.[13,14]

As found in the impedance dimension, the measured impedance was normalized by the specimen thickness and electrode area. Therefore, the grain-boundary resistivity (ρ_{gb}), which was deconvoluted from the impedance spectrum, is different from the specific grain boundary resistivity (ρ_{gb}^{sp}). However, the determination of the ρ_{gb}^{sp} value requires an accurate shape factor for the grain-boundary phase, which is difficult to determine. Instead of ρ_{gb}^{sp}, we simply calculated the resistance per unit grain-boundary area (R_{gbs}) for a specific comparison using the equation, $R_{gbs} = \rho_{gb}/D$, where D is the grain-boundary density (the reciprocal of average grain size).[3] The calculated R_{gbs} values are plotted in Fig. 2(c). The average grain size was the same throughout the specimen, which means that the profile of R_{gbs} was identical to that of ρ_{gb}.

The R_{gbs} value was high at the surface. It decreased abruptly at the second electrodes from the surface and then became saturated at 25–15 Ω cm^2 when the distance from the surface exceeds 2 mm. This clearly shows that the distribution of the grain-boundary conduction can be estimated by the present technique. The grain

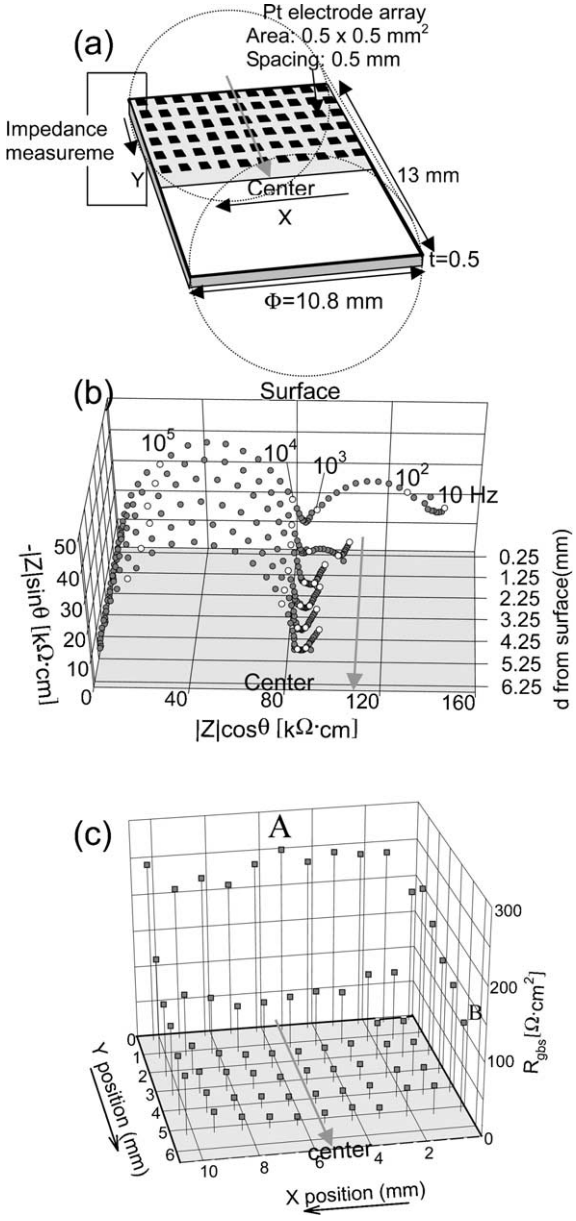

Fig. 2. (a) Schematic diagram of the two-dimensional array of electrodes for measuring the local impedance. (b) The impedance spectra of the C1650 specimen measured at 400 °C in air as a function of the distance from the surface along the cylinder axis. (c) The distribution of the resistance per unit grain-boundary area as a function of specimen location.

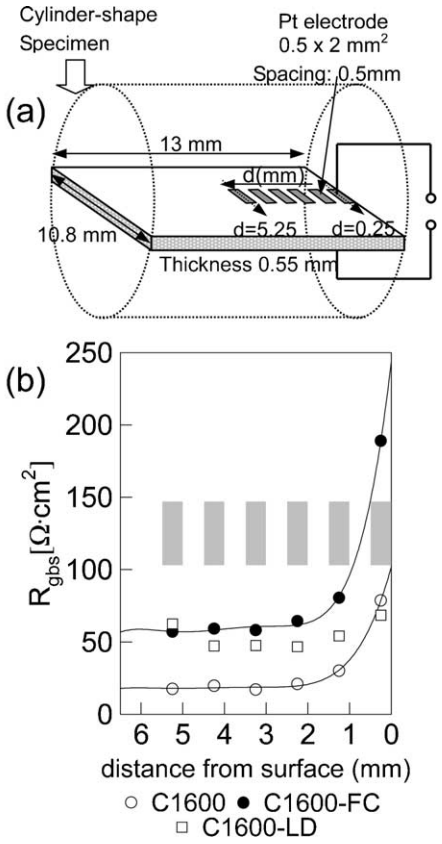

Fig. 3. (a) Schematic diagram of the one-dimensional electrode array. (b) The profiles of the resistance per unit grain boundary area (R_{gbs}) as a function of distance from the surface for the C1600, C1600-FC, and C1600-LD specimens. (see the specimen specification in Table 1).

boundary at the surface was 10–15 times more resistive than that at the center and the most resistive skin layer was approximately 2 mm thick. TEM observations of the previous report revealed that the liquid at the surface was not only more abundant but was also more wettable compared to that in the center.[10] Therefore, the electrically heterogeneous grain boundary could be attributed to the different configurations of the resistive intergranular liquid between the surface and the center. The R_{gbs} value at the surfaces in the radial direction [see point B in Fig. 3(c)] was approximately half that in the axial direction [see point A in Fig. 3(c)]. This appears to emanate from the anisotropy in the sample dimensions and compact densities along the axial and radial directions from the center.

Another array of electrodes was made along the axial direction of the specimen as shown in Fig. 3(a). Fig. 3(b) shows the R_{gbs} profiles for the C1600, C1600-FC, C1600-LD samples, respectively. The R_{gbs} value in the C1600 specimen decreased with increasing the distance from the surface (d) although the variation is small compared to that of the C1650 sample. On the other hand, the fast cooling of the specimen significantly moved the total profile upward, which means an increase in the average grain-boundary resistance of the entire specimen. In contrast to the present result, Badwal and Drennan [15] reported that fast cooling decreased the grain-boundary resistivity in yttria-containing tetragonal zirconia and suggested the relocation of the grain-boundary phase as the cause. In the present study, the change in the wetting behavior and/or crystallization can be considered as feasible reasons. The configuration of the intergranular phase can be changed dynamically during cooling because the wetting/dewetting characteristics are dependent upon temperature. Therefore, quenching after heat-treatment temperature is usually employed to examine the intergranular-phase configuration at high temperatures. Thus, a high R_{gbs} value at the fast cooling rate might occur when the high-temperature configuration of the intergranular liquid is more resistive. The second possibility is the crystallization of the intergranular liquid. Slower cooling from a glass melt usually result in more crystallization when the cooling schedule passed through the crystallization region in the T–T–T (time–temperature–transformation) curve. Therefore, slow cooling can also ease grain boundary conduction by making the intergranular liquid phase less connective via crystallization.

The compact density of the green body is also known to influence the liquid redistribution.[16] The green body without isostatic pressing was sintered to investigate this possibility. The R_{gbs} profile of the C1600-LD specimens was relatively uniform compared to those in the C1600 and C1600-FC specimens. In a previous report, it was suggested that a highly resistive grain boundary at the surface was due to the outward flow of liquid from the center of a specimen by densification.[17] The results in this study show a good correlation between the liquid redistribution and densification. Moreover, the grain-boundary resistance is known to vary according to its thermal history, [15] sintering atmosphere, [18] etc. This suggests that the spatially resolved impedance technique can be a useful tool for understanding the overall change in grain-boundary conduction induced by a local conductivity variation.

5. Conclusions

The spatially heterogeneous distribution of an intergranular liquid was estimated in a 1-mol%-Al_2O_3-doped 15 mol% calcia-stabilized zirconia specimen by a local impedance technique using an array of milli-scale electrodes. The grain boundaries near the surface were significantly more resistive compared to those in the center, which was attributed to the outward rearrangement of the liquid phase. In addition, the overall profile of the grain-boundary resistivity moved upward and was flattened by the fast cooling after sintering and the loose compaction of green body, respectively. This means that millicontact impedance spectroscopy is a useful tool for investigating local variations in grain-boundary conduction.

References

1. Bonanos, N., Steele, B. C. H., Butler, E. P., Johnson, W. B., Worrell, W. L., Macdonald, D. D. and McKubre, M. C. H., Application of impedance spectroscopy. In *Impedance Spectroscopy*, ed. J. R. Macdonald. Wiley, New York, 1987, pp. 191–316.
2. Dijk, T. and van Burggraaf, A. J., Grain boundary effects on ionic conductivity in ceramic $Gd_xZr_{1-x}O_{2-(x/2)}$ solid solutions. *Phys. Stat. Sol. (a)*, 1981, **63**, 229.
3. Miyayama, M., Yanagida, H. and Asada, A., Effect of Al_2O_3 addition on resistivity and microstructure of yttria-stabilized zirconia. *Am. Ceram. Soc. Bull.*, 1986, **65**, 660–664.
4. Rodewald, S., Fleig, J. and Maier, J., Measurement of conductivity profiles in acceptor-doped strontium titanate. *J. Eur. Ceram. Soc.*, 1999, **19**, 797–801.
5. Sánchez-Herencia, A. J., Moreno, R. and Jurado, J. R., Electrical transport properties in zirconia/alumina functionally graded materials. *J. Eur. Ceram. Soc.*, 2000, **20**, 1611–1620.
6. Fleig, J., Rodewald, S. and Maier, J., Spatially resolved measurements of highly conductive and highly resistive grain boundaries using microcontact impedance spectroscopy. *Solid State Ionics*, 2000, **136-137**, 905–911.
7. Rodewald, S., Fleig, J. and Maier, J., Microcontact impedance spectroscopy at single grain boundaries in Fe-doped $SrTiO_3$ polycrystals. *J. Am. Ceram. Soc.*, 2001, **84**, 521–530.
8. Skapin, A. S., Jamnik, J. and Pejovnik, S., Grain boundary conductance in AgCl by micro-contact impedance spectroscopy. *Solid State Ionics*, 2000, **133**, 129–138.
9. Gödickemeier, M., Michel, B., Orliukas, A., Bohac, P., Sasaki, K., Gauckler, L., Heinrich, H., Schwander, P., Kostroz, G., Hofmann, H. and Frei, O., *J. Mater. Res.*, 1994, **9**, 1228–1240.

10. Lee, J.-H., Lee, J. H. and Kim, D.-Y., The inhomogeneity of grain-boundary resistivity in calcia-stabilized zirconia. *J. Am. Ceram. Soc.*, 2002, **85**, 1622–1624.
11. Fisher, C. A. and Matsubara, H., The influence of grain boundary misorientation on ionic conductivity in YSZ. *J. Eur. Ceram. Soc.*, 1999, **19**, 703–707.
12. De Souza, D. P. E. and De Souza, M. F., Liquid phase sintering of Re_2O_3: YSZ ceramics, Part I Grain growth and expelling of the grain boundary glass phase. *J. Mater. Sci.*, 1999, **34**, 4023–4030.
13. Aoki, M., Chiang, Y.-M., Kosacki, I., Lee, J.-R., Tuller, H. and Liu, Y., Solute segregation and grain-boundary impedance in high purity stabilized zirconia. *J. Am. Ceram. Soc.*, 1996, **79**, 1169–1180.
14. Lee, J.-H., Mori, T., Li, J.-G., Ikegami, T., Komatsu, M. and Haneda, H., Improvement of grain-boundary conductivity of 8 mol% yttria-stabilized zirconia by precursor scavenging of siliceous phase. *J. Electrochem. Soc.*, 2000, **147**, 2822–2829.
15. Badwal, S. P. S. and Drennan, J., Grain boundary resistivity in Y-TZP materials as a function of thermal history. *J. Mater. Sci.*, 1989, **24**, 88–96.
16. Shaw, T. M., Liquid redistribution during liquid-phase sintering. *J. Am. Ceram. Soc.*, 1986, **69**, 27–34.
17. Lee, J.-H., Lee, J. H., Jung, Y.-S. and Kim, D.-Y., Effect of Al_2O_3 addition on the distribution of intergranular-liquid phase during sintering of 15 mol% calcia-stabilized zirconia, *J. Am. Ceram. Soc.*, submitted.
18. Badwal, S. P. S. and Hushes, A. E., The effect of sintering atmosphere on impurity phase formation and grain boundary resistivity in Y_2O_3-fully stabilized ZrO_2. *J. Eur. Ceram. Soc.*, 1992, **10**, 115–122.